# Bending and Vibration Analysis of a Mindlin Rectangular Nanoplate using Modified Couple Stress Theory and Navier's Solution

**Majid Eskandari Shahraki**
Department of Aerospace Engineering,
Ferdowsi University of Mashhad, Mashhad, Iran
E-mail: mjdeskandari@gmail.com

**Mahmoud Shariati**
Department of Mechanical Engineering,
Ferdowsi University of Mashhad, Mashhad, Iran
E-mail: mshariati44@um.ac.ir

**Naser Asiaban***
Department of Mechanical Engineering,
Ferdowsi University of Mashhad, Mashhad, Iran
E-mail: naser.asiaban@mail.um.ac.ir
*Corresponding author

**Received: 10 February 2021, Revised: 24 June 2021, Accepted: 10 July 2021**

**Abstract:** In this paper, a Mindlin rectangular nanoplate model is developed for the bending and vibration analysis of a graphene nanoplate based on a modified couple stress theory. In order to consider the small scale effects, the modified couple stress theory, with one length scale parameter, is used. In modified couple stress theory, strain energy density is a function of strain tensor, curvature tensor, stress tensor and symmetric part of couple stress tensor. After obtaining the strain and kinetic energy, external work and substituting them in the Hamilton's principle, the main and auxiliary equations of the nanoplate are obtained. Then, by manipulating the boundary conditions the governing equations are solved using Navier approach for bending and vibration of the nanoplate. The bending rates and dimensionless bending values under uniform surface traction and sinusoidal load and different mode frequencies are all obtained for various plate's dimensional ratios and material length scale to thickness ratios. The effect of material length scale, length, width and thickness of the nanoplate on the bending and vibration ratios are investigated and the results are presented and discussed in details.

**Keywords:** Bending, Modified Couple Stress Theory, Mindlin Nanoplate, Navier's Solution, Vibration

**How to cite this paper:** Majid Eskandari Shahraki, Mahmoud Shariati, and Naser Asiaban, "Bending and Vibration Analysis of a Mindlin Rectangular Nanoplate using Modified Couple Stress Theory and Navier's Solution", Int J of Advanced Design and Manufacturing Technology, Vol. 15/No. 1, 2022, pp. 21–28. DOI: 10.30495/admt.2021.1923209.1252.

**Biographical notes**: **Majid Eskandari Shahraki** is currently a PhD student of Aerospace Engineering at Ferdowsi University of Mashhad, Iran. He received his MSc in Mechanical Engineering from IAU Univesity, Khomeini Shahr branch, Isfahan, Iran in 2014. His main research interests is nanomechanics. **Mohmoud Shariati** is a Professor of Mechanical Engineering at Ferdowsi University of Mashhad, Iran. He received his PhD in Mechanical Engineering from Tarbiat Modarres Univesity, Tehran, Iran in 1999. His current research interest includes nanomechanics, experimental mechanics, fatigue and fracture. **Naser Asiaban** is currently a PhD student of Mechanical Engineering at Ferdowsi University of Mashhad, Iran. He received his MSc in Mechanical Engineering from Babol Noshirvani University of Technology (BNUT), Babol, Iran in 2016. His field of research are simulation of liquid composite molding (LCM) processes and renewable energies.

 

## 1 INTRODUCTION

Performing experiments in the atomic and molecular scales are the safest approach for the study of materials in small-scale. In this method, the nanostructures are studied in real dimensions. In this method, in order to determine the mechanical properties of nanostructures the atomic Force Microscopy (AFM) applies different mechanical loads on nanoplates and measures the plate responses. The difficulties of controlling the test conditions at this scale, high economic costs and time-consuming processes are some setbacks of this method. Therefore, it is only used to validate other simple and low-cost methods.

Atomic simulation is another approach for studying small-scale structures. In this method, the behaviors of atoms and molecules are examined by considering the intermolecular and interatomic effects on their motions, which eventually involves the total deformation of the body. In the case of large deformations and multi atomic scales, the computational costs of this approach become unbearable, so it is only used for small deformation problems.

Given the limitations of the aforementioned methods, researchers have been looking for simpler solutions for studying nanostructures. Modeling small-scale structures using continuum mechanics is another approach for this problem. There are a variety of size-dependent continuum theories that consider size effects, some of these theories are; micromorphic theory, microstructural theory, micropolar theory, Kurt's theory, non-local theory, modified couple stress theory and strain gradient elasticity. All of which are the developed notion of classical field theories, which include size effects.

In this paper, Mindlin rectangular nanoplate model is developed for the bending and vibration analysis of a graphene nanoplate based on a modified couple stress theory and the results are presented with new figures and tables.

## 2 MODIFIED COUPLE STRESS THEORY

In 2002, Yang et al. [1] proposed a modified couple stress model by modifying the theory proposed by Toppin [2], Mindlin and Thursten [3], Quitter [4] and Mindlin [5] in 1964. The modified couple stress theory consists of only one material length scale parameter for projection of the size effect, whereas the classical couple stress theory needs two material length scale parameters. In the modified theory, the strain energy density in the three-dimensional vertical coordinates for a body bounded by the volume V and the area Ω [6], is expressed as the follows:

$$U = \frac{1}{2}\int_V \left(\sigma_{ij}\varepsilon_{ij} + m_{ij}\chi_{ij}\right)dV \quad i,j = 1,2,3 \qquad (1)$$

$$\varepsilon_{ij} = \frac{1}{2}(u_{i,j} + u_{j,i}) \qquad (2)$$

$$\chi_{ij} = \frac{1}{2}\left(\theta_{i,j} + \theta_{j,i}\right) \qquad (3)$$

$\chi_{ij}$ and $\varepsilon_{ij}$ are the symmetric parts of the curvature and strain tensors, and $\theta_i$ and $u_i$ are the displacement and the rotational vectors, respectively.

$$\theta = \frac{1}{2}\, Curl\, \boldsymbol{u} \qquad (4)$$

$\sigma_{ij}$, the stress tensor, and $m_{i,j}$, the deviatory part of the couple stress tensor, are defined as:

$$\sigma_{ij} = \lambda\varepsilon_{kk}\delta_{ij} + 2\mu\varepsilon_{ij} \qquad (5)$$

$$m_{i,j} = 2\mu\, l^2\chi_{ij} \qquad (6)$$

Where, $\lambda$ and $\mu$ are the lame constants, $\delta_{ij}$ is the Kronecker delta and $l$ is the material length scale parameter. From Equations (3) and (6) it can be seen that $\chi_{ij}$and $m_{ij}$ are symmetric.

## 3 MINDLIN'S PLATE MODEL

The displacement equations for the Mindlin's plate are defined as:

$$\begin{aligned} u_1(x,y,z,t) &= z\,\varphi_x(x,y,t) \\ u_1(x,y,z,t) &= z\,\varphi_x(x,y,t) \\ u_3(x,y,z,t) &= w(x,y,t) \end{aligned} \qquad (7)$$

Where, $\varphi_x$ and $\varphi_y$ are the rotations of the normal vector around the x and y axis, respectively, and w is the midpoint displacement of the plate in the z-axis direction. The strain and stress tensors, the symmetric part of the curvature tensor, and the rotational vector for the Mindlin's plate are obtained as follows:

$$\varepsilon_{xx} = z\frac{\partial\varphi_x}{\partial x} \qquad (8)$$

$$\varepsilon_{yy} = z\frac{\partial\varphi_y}{\partial y} \qquad (9)$$

$$\varepsilon_{zz} = 0 \qquad (10)$$

$$\varepsilon_{xy} = \varepsilon_{yx} = \frac{1}{2}z\left(\frac{\partial\varphi_x}{\partial y} + \frac{\partial\varphi_y}{\partial x}\right) \qquad (11)$$

$$\varepsilon_{xz} = \varepsilon_{zx} = \frac{1}{2}\left(\frac{\partial w}{\partial x} + \varphi_x\right) \qquad (12)$$

$$\varepsilon_{yz}=\varepsilon_{zy}=\frac{1}{2}\left(\frac{\partial w}{\partial y}+\varphi_y\right) \quad (13)$$

$$\theta_x=\frac{1}{2}\left(\frac{\partial w}{\partial y}-\varphi_y\right) \quad (14)$$

$$\theta_y=\frac{1}{2}\left(\varphi_x-\frac{\partial w}{\partial x}\right) \quad (15)$$

$$\theta_z=\frac{1}{2}z\left(\frac{\partial \varphi_y}{\partial x}-\frac{\partial \varphi_x}{\partial y}\right) \quad (16)$$

$$x_{xx}=\frac{1}{2}\left(\frac{\partial^2 w}{\partial x\,\partial y}-\frac{\partial \varphi_y}{\partial x}\right) \quad (17)$$

$$x_{yy}=\frac{1}{2}\left(\frac{\partial \varphi_x}{\partial y}-\frac{\partial^2 w}{\partial x \partial y}\right) \quad (18)$$

$$x_{zz}=\frac{1}{2}\left(\frac{\partial \varphi_y}{\partial x}-\frac{\partial \varphi_x}{\partial y}\right) \quad (19)$$

$$x_{xy}=\frac{1}{4}\left(\frac{\partial^2 w}{\partial y^2}-\frac{\partial^2 w}{\partial x^2}+\frac{\partial \varphi_x}{\partial x}-\frac{\partial \varphi_y}{\partial y}\right) \quad (20)$$

$$x_{xz}=\frac{1}{4}z\left(\frac{\partial^2 \varphi_y}{\partial x^2}-\frac{\partial^2 \varphi_x}{\partial y\,\partial x}\right) \quad (21)$$

$$x_{yz}=\frac{1}{4}z\left(\frac{\partial^2 \varphi_y}{\partial x \partial y}-\frac{\partial^2 \varphi_x}{\partial y^2}\right) \quad (22)$$

$$\sigma_{xx}=(\lambda+2\mu)\,z\,\frac{\partial \varphi_x}{\partial x}+\lambda\,z\,\frac{\partial \varphi_y}{\partial y} \quad (23)$$

$$\sigma_{yy}=\lambda\,z\,\frac{\partial \varphi_x}{\partial x}+(\lambda+2\mu)\,z\,\frac{\partial \varphi_y}{\partial y} \quad (24)$$

$$\sigma_{zz}=\lambda\left(z\,\frac{\partial \varphi_x}{\partial x}+z\,\frac{\partial \varphi_y}{\partial y}\right) \quad (25)$$

$$\sigma_{yx}=\sigma_{xy}=\mu\,z\left(\frac{\partial \varphi_x}{\partial y}+\frac{\partial \varphi_y}{\partial x}\right) \quad (26)$$

$$\sigma_{xz}=\sigma_{zx}=\mu\left(\frac{\partial w}{\partial x}+\varphi_x\right) \quad (27)$$

$$\sigma_{yz}=\sigma_{zy}=\mu\left(\frac{\partial w}{\partial y}+\varphi_y\right) \quad (28)$$

The variation of the strain energy is expressed as follows:

$$\delta U=\int_V(\sigma_{xx}\,\delta\varepsilon_{xx}+\sigma_{yy}\,\delta\varepsilon_{yy}+2\sigma_{xy}\,\delta\varepsilon_{xy}+2\sigma_{xz}\,\delta\varepsilon_{xz}+2\sigma_{yz}\,\delta\varepsilon_{yz}+m_{xx}\,\delta x_{xx}+m_{yy}\,\delta x_{yy}+m_{zz}\,\delta x_{zz}+2m_{xy}\,\delta x_{xy}+2m_{xz}\,\delta x_{xz}+2m_{yz}\,\delta x_{yz})\,dV \quad (29)$$

For the sake of simplification, the coefficient of each variable in the above equation is named from $F_1$ to $F_{15}$ and this equation can be rewritten as shown below:

$$\delta U=\int_V(F_1\delta w_{,xx}+F_2\,\delta w_{,yy}+F_3\,\delta w_{,xy}+F_4\delta w_{,x}+F_5\,\delta w_{,y}+F_6\,\delta\varphi_{x,yy}+F_7\delta\varphi_{y,xx}+F_8\,\delta\varphi_{y,xy}+F_9\,\delta\varphi_{x,yx}+F_{10}\,\delta\varphi_{x,x}+F_{11}\,\delta\varphi_{y,y}+F_{12}\delta\varphi_{x,y}+F_{13}\,\delta\varphi_{y,x}++F_{14}\,\delta\varphi_x+F_{15}\,\delta\varphi_y)dV \quad (30)$$

Where:

$$F_1=-\frac{1}{4}\mu l^2\left(\frac{\partial^2 w}{\partial y^2}-\frac{\partial^2 w}{\partial x^2}+\frac{\partial \varphi_x}{\partial x}-\frac{\partial \varphi_y}{\partial y}\right) \quad (31)$$

$$F_2=\frac{1}{4}\mu l^2\left(\frac{\partial^2 w}{\partial y^2}-\frac{\partial^2 w}{\partial x^2}+\frac{\partial \varphi_x}{\partial x}-\frac{\partial \varphi_y}{\partial y}\right) \quad (32)$$

$$F_3=\mu l^2\left(\frac{\partial^2 w}{\partial x \partial y}-\frac{1}{2}\frac{\partial \varphi_y}{\partial x}-\frac{1}{2}\frac{\partial \varphi_x}{\partial y}\right) \quad (33)$$

$$F_4=\mu\left(\frac{\partial w}{\partial x}+\varphi_x\right) \quad (34)$$

$$F_5=\mu\left(\frac{\partial w}{\partial y}+\varphi_y\right) \quad (35)$$

$$F_6=F_8=\frac{1}{4}\mu l^2 z^2\left(\frac{\partial^2 \varphi_y}{\partial x \partial y}-\frac{\partial^2 \varphi_x}{\partial y^2}\right) \quad (36)$$

$$F_7=F_9=\frac{1}{4}\mu l^2 z^2\left(\frac{\partial^2 \varphi_y}{\partial x^2}-\frac{\partial^2 \varphi_x}{\partial x \partial y}\right) \quad (37)$$

$$F_{10}=(\lambda+2\mu)z^2\frac{\partial \varphi_x}{\partial x}+\lambda z^2\frac{\partial \varphi_y}{\partial y}+\frac{1}{4}\mu l^2\left(\frac{\partial^2 w}{\partial y^2}-\frac{\partial^2 w}{\partial x^2}+\frac{\partial \varphi_x}{\partial x}-\frac{\partial \varphi_y}{\partial y}\right) \quad (38)$$

$$F_{11}=\lambda Z^2\frac{\partial \varphi_x}{\partial x}+(\lambda+2\mu)z^2\,\frac{\partial \varphi_y}{\partial y} \quad (39)$$

$$-\frac{1}{4}\mu l^2\left(\frac{\partial^2 w}{\partial y^2}-\frac{\partial^2 w}{\partial x^2}+\frac{\partial \varphi_x}{\partial x}-\frac{\partial \varphi_y}{\partial y}\right)F_{12}=\mu z^2\left(\frac{\partial \varphi_x}{\partial y}+\frac{\partial \varphi_y}{\partial x}\right)+\mu l^2\left(\frac{\partial \varphi_x}{\partial y}-\frac{1}{2}\frac{\partial \varphi_y}{\partial x}-\frac{1}{2}\frac{\partial^2 w}{\partial x \partial y}\right) \quad (40)$$

$$F_{13}=\mu z^2\left(\frac{\partial \varphi_x}{\partial y}+\frac{\partial \varphi_y}{\partial x}\right)+\mu l^2\left(\frac{\partial \varphi_y}{\partial x}-\frac{1}{2}\frac{\partial^2 w}{\partial x \partial y}-\frac{1}{2}\frac{\partial \varphi_x}{\partial y}\right) \quad (41)$$

$$F_{14}=\mu\left(\frac{\partial w}{\partial x}+\varphi_x\right) \quad (42)$$

$$F_{15}=\mu\left(\frac{\partial w}{\partial y}+\varphi_y\right) \quad (43)$$

## 4 VIRTUAL WORK OF THE EXTERNAL FORCES

In these kind of problems, the virtual work of three kinds of external forces are included in the solutions, if the middle-plane and the middle-perimeter of the plate are shown as Ω and Γ respectively, these virtual works are [7]:

1- The virtual work done by the body forces, which is applied on the volume V= Ω× (- h⁄2, h⁄2).
2- The virtual work done by the surface tractions at the upper and lower surfaces (Ω).
3- The virtual work done by the shear tractions on the lateral surfaces, S= Γ× (- h⁄2, h⁄2).
If ($f_x$, $f_y$, $f_z$) are the body forces, ($c_x$, $c_y$, $c_z$) are the body couples, ($q_x$, $q_y$, $q_z$) are the forces acting on the Ω plane, ($t_x$, $t_y$, $t_z$) are the Cauchy's tractions and ($S_x$, $S_y$, $S_z$) are surface couples, the Variations of the virtual work is expressed as:

$$\delta w=-\left[\int_{\Omega}(f_x\delta u+f_y\delta V+f_z\delta w+q_x\delta u+q_y\delta V +q_z\delta w+c_x\delta\theta_x+c_y\,\delta\theta_y+c_z\delta\theta_z)\,dx\,dy + \int_{\Gamma}(t_x\delta u+t_y\delta V+t_z\delta w+s_x\theta_x\ +s_y\delta\theta_y+s_z\delta)\right. \quad (44)$$

Given that in this study only the external force $q_z$ was applied, virtual work becomes:

$$\delta w=\int_0^a\int_0^b q(x,y)\delta w(x,y)dx\,dy \quad (45)$$

The variation of kinetic energy is obtained as:

$$\delta T=\int_A\int_{-\frac{h}{2}}^{\frac{h}{2}}\rho(\dot u_1\delta\dot u_1+\dot u_2\delta\dot u_2+\dot u_3\delta\dot u_3)dA\,dz=\int_A\left[\rho h\dot w\delta\dot w+\frac{\rho h^3}{12}\left(\dot\varphi_X\delta\dot\varphi_X+\dot\varphi_y\delta\dot\varphi_y\right)\right]dA \quad (46)$$

Where, ρ is the density.
Finally using the Hamilton's principle, it can be said that [8]:

$$\int_0^T\left(\delta T-(\delta U-\delta w)\right)dt=0 \quad (47)$$

Where, T is the kinetic energy, U is the strain energy, and W is the work of the external forces.

## 5 THE GOVERNING EQUATIONS OF THE PLATE

Using Hamilton's principle, Equation (47), and the Equations from (44) to (46), the governing Equations of the plate including the external forces are obtained as follows:

$$\left[\int_{-h/2}^{h/2}\left(\frac{\partial^2F_1}{\partial x^2}-\frac{\partial F_4}{\partial x}+\frac{\partial^2F_2}{\partial y^2}+\frac{\partial^2F_3}{\partial x\partial y}-\frac{\partial F_5}{\partial y}\right)dz\right] \quad (48)$$

$$=q(x,y)+\rho h\,\frac{\partial^2w}{\partial t^2}\int_{-h/2}^{h/2}\left(\frac{\partial^2F_6}{\partial y^2}+\frac{\partial^2F_9}{\partial x\partial y}-\frac{\partial F_{12}}{\partial y}-\frac{\partial F_{10}}{\partial x}+F_{14}\right)dz=\frac{\rho h^3}{12}\,\frac{\partial^2\varphi_x}{\partial t^2} \quad (49)$$

$$\int_{-h/2}^{h/2}\left(\frac{\partial^2F_7}{\partial x^2}-\frac{\partial F_{13}}{\partial x}+\frac{\partial^2F_8}{\partial x\partial y}-\frac{\partial F_{11}}{\partial y}+F_{15}\right)dz=\frac{\rho h^3}{12}\,\frac{\partial^2\varphi_y}{\partial t^2} \quad (50)$$

## 6 THE GENERAL GOVERNING EQUATION OF THE MINDLIN'S PLATE (INCLUDING VIBRATION AND BENDING)

Considering the following constants:

$$\begin{array}{lll} C_1=\frac{1}{4}\mu l^2h & C_2=\mu h\,k_s & C_3=\frac{1}{4}\mu l^2I_2 \\ & C_5=-\lambda I_2 & C_6=-\mu I_2-\lambda I_2 \\ C_4=-\mu I_2-\mu l^2h & -2\mu I_2-\frac{1}{4}\mu l^2h & +\frac{3}{4}\mu l^2h \\ C_7=\rho h & C_8=\frac{\rho h^3}{12} & k_s=\frac{5}{6}=0.8 \end{array} \quad (51)$$

Where,

$$I_i=\int_{-\frac{h}{2}}^{\frac{h}{2}}Z^i\,dz \quad (52)$$

The general governing equation of the Mindlin's plate will becomce:

$$2C_1\frac{\partial^4w}{\partial x^2\partial y^2}+C_1\frac{\partial^4w}{\partial x^4}+C_1\frac{\partial^4w}{\partial y^4}-C_2\frac{\partial^2w}{\partial x^2}-C_2\frac{\partial^2w}{\partial y^2}-C_1\frac{\partial^3\varphi_x}{\partial x^3} \quad (53)$$

$$-C_1\frac{\partial^3\varphi_y}{\partial y^3}-C_1\frac{\partial^3\varphi_y}{\partial x^2\partial y}-C_2\frac{\partial\varphi_X}{\partial x}-C_2\frac{\partial\varphi_y}{\partial y}=q(x,y)+C_7\frac{\partial^2w}{\partial t^2}$$

$$C_3\left(\frac{\partial^4\varphi_y}{\partial x\partial y^3}-\frac{\partial^4\varphi_x}{\partial y^4}+\frac{\partial^4\varphi_y}{\partial x^3\partial y}-\frac{\partial^4\varphi_x}{\partial x^2\partial y^2}\right)+C_4\,\frac{\partial^2\varphi_x}{\partial y^2} \quad (54)$$

$$+C_5\frac{\partial^2\varphi_x}{\partial x^2}+C_6\frac{\partial^2\varphi_y}{\partial x\partial y}+C_1\frac{\partial^3w}{\partial x\,\partial y^2}+C_1\frac{\partial^3w}{\partial x^3}$$

$$+C_2\frac{\partial w}{\partial x}+C_2\varphi_x=C_8\frac{\partial^2\varphi_x}{\partial t^2}$$

$$C_3\left(\frac{\partial^4\varphi_y}{\partial x^4}-\frac{\partial^4\varphi_x}{\partial x^3\partial y}+\frac{\partial^4\varphi_y}{\partial x^2\partial y^2}-\frac{\partial^4\varphi_x}{\partial x\partial y^3}\right)+C_6\,\frac{\partial^2\varphi_x}{\partial x\partial y}$$

$$+C_4\frac{\partial^2\varphi_y}{\partial x^2}+C_5\frac{\partial^2\varphi_y}{\partial y^2}+C_1\frac{\partial^3w}{\partial y\partial x^2} \quad (55)$$

$$+C_1\frac{\partial^3w}{\partial y^3}+C_2\frac{\partial w}{\partial y}+C_2\varphi_x=C_8\frac{\partial^2\varphi_y}{\partial t^2}$$

## 7 SOLUTION OF THE GOVERNING EQUATIONS USING NAVIER'S METHOD

The Navier's solution is applicable to the rectangular plates which have simply supported boundary conditions on all edges. Since the boundary conditions are spontaneously satisfied in this method, the unknown

functions of the plate's mid-plane were assumed to be double trigonometric series [7], [9]:

$$W(x,y,t)=\sum_{m=1}^{\infty}\sum_{n=1}^{\infty} W_{mn}\sin\alpha x\sin\beta y\, e^{i\omega t} \quad (56)$$

$$\varphi_x(x,y,t)=\sum_{m=1}^{\infty}\sum_{n=1}^{\infty} X_{mn}\cos\alpha x\sin\beta y\, e^{i\omega t} \quad (57)$$

$$\varphi_y(x,y,t)=\sum_{m=1}^{\infty}\sum_{n=1}^{\infty} y_{mn}\sin\alpha x\cos\beta y\, e^{i\omega t} \quad (58)$$

The force can also be calculated from the following relations:

$$q=\sum_{m=1}^{\infty}\sum_{n=1}^{\infty} Q_{mn}\sin\alpha x\sin\beta y\, e^{i\omega t} \quad (59)$$

$$Q_{mn}=\frac{4}{ab}\int_0^a\int_0^b q(x,y)\sin\alpha x\sin\beta y\,dx\,dy \quad (60)$$

$$Q_{mn}=\begin{cases} q_0 & ;\text{For sinusoidal force}\\ \frac{16q_0}{mn\pi^2} & ;\text{For uniform force}\\ \frac{4Q_0}{ab} & ;\text{For point force in the plane center}\end{cases} \quad (61)$$

Where:

$$\alpha=\frac{\pi m}{a}\ ,\ \beta=\frac{\pi n}{b}\ ,\ i=\sqrt{-1} \quad (62)$$

Simply-supported boundary conditions were also satisfied by the Navier's method according to the following equations:

$$x=0,\ x=a\begin{cases} w(0,y)=w(a,y)=\sum\sum w_{mn}\sin\frac{m\pi}{a}x\sin\frac{n\pi}{b}y=0\\ \varphi_y(0,y)=\varphi_y(a,y)=\sum\sum y_{mn}\sin\frac{m\pi}{a}x\cos\frac{n\pi}{b}y=0\end{cases} \quad (63)$$

$$y=0,\ y=b\begin{cases} w(x,0)=w(x,b)=\sum\sum w_{mn}\sin\frac{m\pi}{a}x\sin\frac{n\pi}{b}y=0\\ \varphi_x(x,0)=\varphi_x(x,b)=\sum\sum X_{mn}\cos\frac{m\pi}{a}x\sin\frac{n\pi}{b}y=0\end{cases} \quad (64)$$

## 8 THE GENERAL EQUATION MATRIX OF A MINDLIN'S PLANE

After solving the governing equations and naming the coefficient of each variable, we have:

$$U_1=2C_1\alpha^2\beta^2+C_1\alpha^4+C_1\beta^4+C_2\alpha^2+C_2\beta^2 \quad (65)$$

$$U_2=U_4=-C_1\alpha^3-C_1\alpha\beta^2+C_2\alpha \quad (66)$$

$$U_3=U_7=-C_1\beta^3-C_1\alpha^2\beta+C_2\beta \quad (67)$$

$$U_5=-C_3\beta^4-C_3\alpha^2\beta^2-C_4\beta^2-C_5\alpha^2+C_2 \quad (68)$$

$$U_6=C_3\alpha\beta^3+C_3\alpha^3\beta-C_6\alpha\beta \quad (69)$$

$$U_8=-C_3\alpha^3\beta-C_3\alpha\beta^3-C_6\alpha\beta \quad (70)$$

$$U_9=C_3\alpha^4+C_3\alpha^2\beta^2-C_4\alpha^2-C_5\beta^2+C_2 \quad (71)$$

$$K_1=-C_7 \quad (72)$$

$$K_2=K_3=K_4=K_6=K_7=K_8=0 \quad (73)$$

$$K_5=K_9=-C_8 \quad (74)$$

Finally, the general equation matrix of the Mindlin's plate along with the auxiliary equations will be obtained as follows:

$$\left(\begin{bmatrix}U_1&U_2&U_3\\U_4&U_5&U_6\\U_7&U_8&U_9\end{bmatrix}-\omega^2\begin{bmatrix}K_1&K_2&K_3\\K_4&K_5&K_6\\K_7&K_8&K_9\end{bmatrix}\right)\begin{bmatrix}w_{mn}\\X_{mn}\\y_{mn}\end{bmatrix}=\begin{bmatrix}Q_{mn}\\0\\0\end{bmatrix} \quad (75)$$

Various materials such as epoxy, graphene, copper and so on can be considered as the plate's material. In this study, graphene is chosen as the plate's material. A single-layer graphene plate has the following properties [8]:

$$E=1.06\text{TPa},\ \nu=0.25\ ,\ h=0.34\text{nm},\ \rho=2250\ {}^{kg}/_{m^3} \quad (76)$$

Also, the relationship between E, μ and ν can be expressed as:

$$\lambda=\frac{\nu E}{(1+\nu)(1-2\nu)}\ ,\ \mu=\frac{E}{2(1+\nu)} \quad (77)$$

Where, μ and λ are the lame's coefficients and E is the Young's modulus [10]. The value of the distributed force was considered to be $q = 1N/m^2$.

## 9 RESULTS AND DISCUSSION

Results were obtained using a computational program coded in the MATLAB software. The results have also been compared with the literature [11-13] and good agreements between results were observed. The plate's dimensional parameters are chosen as follows:

a: plate's length
b: plate's width
h: plate's thickness
l: material length scale parameter

Table 1 shows the Mindlin's nanoplate bending rate under uniform surface traction for different material length scale parameters to thickness (l/h) and length to width ratio (a/b). As can be seen, as the length scale parameter to thickness ratio increases, the bending ratio decreases but it increases due to the increase in the plate's length to width ratio.

**Table 1** The Mindlin's nanoplate bending rate under surface traction for different length to width and material length scale to thickness ratios (q=1e-18 N/nm$^2$, a/h=30)

| a/b | l/h | | | |
|---|---|---|---|---|
| | 0 | 0.5 | 1 | 2 |
| 1 | 10.7687 | 2.5368 | 0.776721 | 0.212569 |
| 1.5 | 20.7503 | 4.88668 | 1.49283 | 0.404766 |
| 2 | 27.9754 | 6.58762 | 2.0112 | 0.543936 |

Figure 1 compares the bending values of different nanoplates under the sinusoidal load for different length to width and material length scale parameters to thickness ratios. It is clear that as the length scale parameter to thickness ratio increases, the bending ratio decreases but it increases due to the increase in the plate's aspect ratio.

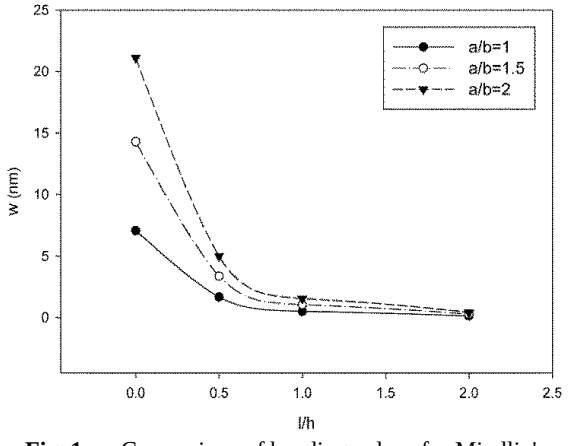


**Fig. 1** Comparison of bending values for Mindlin's nanoplates under the sinusoidal load for different length to width and material length scale to thickness ratios (q=1e-18 N/nm$^2$, a/h=30).

Table 2 shows the dimensionless bending values of different nanoplates under the sinusoidal load for different length to width ratios.

**Table 2** The dimensionless bending values of different nanoplates under the sinusoidal load for different length to width ratios (l/h=1, a/h=30, q=1e-18 N/nm$^2$)

| a/b | Kirchhoff plate | Mindlin plate | Third order shear deformation plate | N order shear deformation plate (n=5) |
|---|---|---|---|---|
| 1 | 0.2 | 0.072264 | 0.19912 | 0.19907 |
| 1.5 | 0.2 | 0.072121 | 0.19927 | 0.19923 |
| 2 | 0.2 | 0.072049 | 0.19935 | 0.19931 |

As shown in the table, the dimensionless bending values were the highest for the Kirchhoff's nanoplate and the lowest for Mindlin's nanoplate. Tables 3 to 6 show that frequencies of Mindlin's nanoplate different vibration modes $(\omega_{11} - \omega_{12} - \omega_{21} - \omega_{22})$ decrease due to increase in length to width ratio.

**Table 3** Comparison of the first mode frequencies $(\omega_{11})$ of Mindlin's nanoplate for different length to width and length scale parameter to thickness ratio (a/b=1, h=0.34)

| l/h | a/h | | | |
|---|---|---|---|---|
| | 20 | 30 | 40 | 50 |
| 0 | 31.2102 | 13.9429 | 7.8572 | 5.0329 |
| 0.5 | 64.2570 | 28.7266 | 16.1924 | 10.3732 |
| 1 | 115.4757 | 51.9052 | 29.3145 | 18.7965 |
| 2 | 215.5686 | 99.1252 | 56.4382 | 36.3253 |

**Table 4** Comparison of the mode frequencies $(\omega_{12})$ of Mindlin's nanoplate for different length to width and length scale parameter to thickness ratio (a/b=1, h=0.34)

| a/h | l/h | | | |
|---|---|---|---|---|
| | 0 | 0.5 | 1 | 2 |
| 20 | 76.9722 | 158.2169 | 280.4153 | 492.9660 |
| 30 | 34.6425 | 71.3140 | 128.0217 | 237.9174 |
| 40 | 19.5743 | 40.3193 | 72.7219 | 137.8488 |
| 50 | 12.5539 | 25.8663 | 46.7575 | 89.4593 |

**Table 5** Comparison of the mode frequencies $(\omega_{21})$ of Mindlin's nanoplate for different length to width and length scale parameter to thickness ratio (a/b=1, h=0.34)

| a/h | l/h | | | |
|---|---|---|---|---|
| | 0 | 0.5 | 1 | 2 |
| 20 | 76.9722 | 158.2169 | 280.4153 | 492.9660 |
| 30 | 34.6425 | 71.3140 | 128.0217 | 237.9174 |
| 40 | 19.5743 | 40.3193 | 72.7219 | 137.8488 |
| 50 | 12.5539 | 25.8663 | 46.7575 | 89.4593 |

**Table 6** Comparison of the mode frequencies $(\omega_{22})$ of Mindlin's nanoplate for different length to width and length scale parameter to thickness ratio (a/b=1, h=0.34)

| a/h | l/h | | | |
|---|---|---|---|---|
| | 0 | 0.5 | 1 | 2 |
| 20 | 121.5505 | 249.5297 | 436.5378 | 722.2379 |
| 30 | 55.0918 | 113.3246 | 202.1703 | 365.8010 |
| 40 | 31.2102 | 64.2570 | 115.4757 | 215.5686 |
| 50 | 20.0412 | 41.2804 | 74.4444 | 141.0270 |

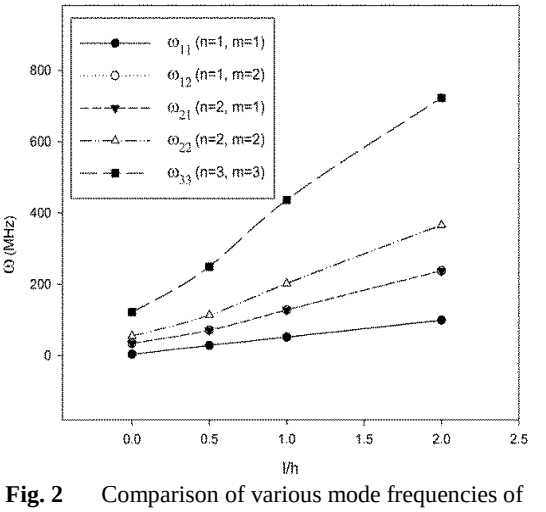


**Fig. 2** Comparison of various mode frequencies of Mindlin's nanoplate for different length scale parameter to thickness ratio (a/b=1, h=0.34, a/h=30).

Also, for the classical theory (neglecting the effect of size parameter), the frequency reaches its lowest value, but with an increase in the size effect, the frequency value increases. It was also observed that the first mode has the lowest frequency value and it increases for the next modes. Figure 2 shows that frequencies of Mindlin's nanoplate different vibration modes increase due an increase in length scale parameter to thickness ratio. By comparing "Figs. 2-3", it can be observed that the vibration frequency decreases due to an increase in nanoplate aspect ratio. This fact can also be found by comparing "Tables 7-8".

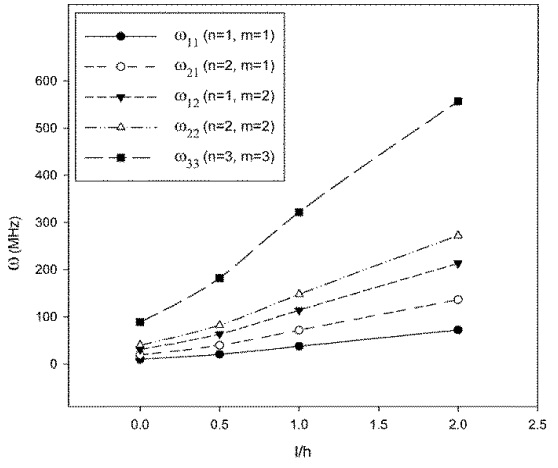


**Fig. 3** Comparison of various mode frequencies of Mindlin's nanoplate for different length scale parameter to thickness ratio (a/b=1.5, h=0.34, a/h=30).

**Table 7** Comparison of different mode frequencies of Mindlin's nanoplate for various length to width ratios (a/b=0.5, h=0.34, l/h=1)

| Mode | a/h | | | |
|---|---|---|---|---|
| | 20 | 30 | 40 | 50 |
| $\omega_{11}$ | 280.4153 | 128.0217 | 72.7219 | 46.7575 |
| $\omega_{12}$ | 436.5378 | 202.1703 | 115.4757 | 74.4444 |
| $\omega_{21}$ | 860.2980 | 413.9252 | 240.0504 | 155.9272 |
| $\omega_{22}$ | 988.5087 | 481.2484 | 280.4153 | 182.5827 |
| $\omega_{33}$ | 1844.9056 | 988.5087 | 596.8069 | 395.7091 |

**Table 8** Comparison of different mode frequencies of Mindlin's nanoplate for various length to width ratios (a/b=1, h=0.34, l/h=1)

| Mode | a/h | | | |
|---|---|---|---|---|
| | 20 | 30 | 40 | 50 |
| $\omega_{11}$ | 115.4757 | 51.9052 | 29.3145 | 18.7965 |
| $\omega_{12}$ | 280.4153 | 128.0217 | 72.7219 | 46.7575 |
| $\omega_{21}$ | 280.4153 | 128.0217 | 72.7219 | 46.7575 |
| $\omega_{22}$ | 436.5378 | 202.1703 | 115.4757 | 74.4444 |
| $\omega_{33}$ | 903.7094 | 436.5378 | 253.5674 | 164.8397 |

Table 9 shows the frequencies of various nanoplates different vibration modes $(\omega_{11} - \omega_{12} - \omega_{21} - \omega_{22})$. According to the table, the Mindlin's nanoplate has the highest and third order nanoplate has the lowest frequency values.

**Table 9** Comparison of dimensionless frequencies of different modes of various nanoplates for length to thickness ratio (a/b=1, l/h=1)

| Mode | a/h | | | |
|---|---|---|---|---|
| | 10 | 20 | 30 | 40 |
| **Mindlin plate** | | | | |
| $\omega_{11}$ | 436.5378 | 115.4757 | 51.9052 | 29.3145 |
| $\omega_{12}$ | 988.5087 | 280.4153 | 128.0217 | 72.7219 |
| $\omega_{21}$ | 988.5087 | 280.4153 | 128.0217 | 72.7219 |
| $\omega_{22}$ | 1444.5250 | 436.5378 | 202.1703 | 115.4757 |
| **Kirchhoff plate** | | | | |
| $\omega_{11}$ | 279.48251 | 70.29855 | 31.27940 | 17.60169 |
| $\omega_{12}$ | 690.3772 | 175.2090 | 78.0917 | 43.9704 |
| $\omega_{21}$ | 690.3772 | 175.2090 | 78.0917 | 43.9704 |
| $\omega_{22}$ | 1091.7424 | 279.4825 | 124.7766 | 70.2985 |
| **Third order shear deformation plate** | | | | |
| $\omega_{11}$ | 276.5826 | 70.1049 | 31.2407 | 17.5894 |
| $\omega_{12}$ | 674.3836 | 174.0385 | 77.8533 | 43.8941 |
| $\omega_{21}$ | 674.3836 | 174.0385 | 77.8533 | 43.8941 |
| $\omega_{22}$ | 1055.3211 | 276.5826 | 124.1752 | 70.1049 |

## 10 CONCLUSION

In this study, the bending and vibration of a graphene Mindlin's nanoplate were investigated using the modified couple stress theory. As observed in the tables and figures, the Mindlin's nanoplate bending rate under uniform surface traction, decreases with an increase in the material length scale to thickness ratio of the nanoplate, but, this value increases with an increase in the aspect ratio of the nanoplate. Furthermore, by comparing different nanoplates under uniform surface traction, it was found that the Mindlin's nanoplate yields the lowest and the Kirchhoff's nanoplate yields the highest values for dimensionless bending.

Analysis of frequencies of different modes for Mindlin's nanoplate showed that this value decreases due to an increase in length to thickness ratio. Also, for the classical theory (neglecting the effect of size parameter), the frequency reaches its lowest value, but with an increase in the size effect, the dimensionless frequency values increases. It was also found that the Mindlin's nanoplate yields the highest and the third-order nanoplate yields the lowest values for frequency.

## REFERENCES

[1] Yang, F., Chong, A. C. M., Lam, D. C. C., and Tong, P., Couple Stress Based Strain Gradient Theory for Elasticity, Int. J. Solids Struct, No. 39, 2002, pp. 2731–2743, DOI: 10.1016/S0020-7683(02)00152-X.

[2] Toupin, R. A., Elastic Materials with Couple Stresses, Arch. Rational Mech. Anal, No. 11, 1962, pp. 385–414.

[3] Mindlin, R. D., Tiersten, H. F., Effects of Couple-Stresses in Linear Elasticity, Arch. Rational Mech. Anal, No. 11, 1962, pp. 415–448.

[4] Koiter, W. T., Couple Stresses in the Theory of Elasticity, I and II Proc K. Ned. Akad, Wet. (B), No. 67, 1964, pp. 17–44.

[5] Mindlin, R. D., Micro-Structure in Linear Elasticity, Arch. Rational Mech. Anal, No. 16, 1964, pp. 51–78.

[6] Tsiatas. G. C., A New Kirchhoff Model Based On a Modified Couple Stress Theory, International Journal of Solids and Structures, No. 46, 2009, pp. 2757-2764, DOI: 10.1016/j.ijsolstr.2009.03.004.

[7] Tai. T., HoChoi. D., Size-Dependent Functionally Graded Kirchhoff and Mindlin Plate Theory Based on a Modified Couple Stress Theory, Composite Structures, No. 95, 2013, pp. 142-153, DOI: 10.1016/j.compstruct.2012.08.023.

[8] Akgoz, B., Civalek, O., Free Vibration Analysis for Single –Layered Graphene Sheets in an Elastic Matrix Via Modified Couple Stress Theory, Materials and Design, No. 42, 2012, pp. 164-171, DOI: 10.1016/j.matdes.2012.06.002.

[9] Wang. B., Zhou. S., Zhao, J., and Chen, X., Asize-Dependent Kirchhoff Micro-Plate Model Based on Strain Gradient Elasticity Theory, European Journal of Mechanics A/Solids, No. 30, 2011, pp. 517-524, DOI: 10.1016/j.euromechsol.2011.04.001.

[10] Roque, C. M. C., Ferreira, A. J. M., and Reddy. J. N., Analysis of Mindlin Micro Plates with A Modified Couple Stress Theory and Meshlessmethod, Applied Mathematical Modeling, No. 37, 2013, pp. 4626-4633, DOI: 10.1016/j.apm.2012.09.063.

[11] Thai, H. T., Kim, S. E., A Size-Dependent Functionally Graded Reddy Plate Model Based on a Modified Couple Stress Theory, Composites Part B: Engineering, Vol. 45, 2013, pp. 1636-1645, DOI:10.1016/j.compositesb.2012.09.065.

[12] Lou, J., He, L., and Du, J., A Unified Higher Order Plate Theory for Functionally Graded Microplates Based On the Modified Couple Stress Theory, Composite Structures, No. 133, 2015, pp. 1036-1047, DOI: 10.1016/j.compstruct.2015.08.009.

[13] Xiang, S., Kang, G. W., A Nth-Order Shear Deformation Theory for The Bending Analysis On the Functionally Graded Plates, European Journal of Mechanics - A/Solids, No. 37, 2013, pp. 336-343, DOI: 10.1016/j.euromechsol.2012.08.005.